

TERAHERTZ SPIRAL PLANAR GOUBAU LINE REJECTORS FOR BIOLOGICAL CHARACTERIZATION

A. Treizebre, M. Hofman, and B. Bocquet

Institute of Electronics, Microelectronics and Nanotechnology
University of Lille 1, F59652 Villeneuve dAscq, France

Abstract—Terahertz spectroscopy brings precious complementary information in life science by probing directly low energy bindings inside matter. This property has been demonstrated on dehydrated substances, and interesting results are obtained on liquid solutions. The next step is the characterization of living cells. We have successfully integrated THz passive circuits inside Biological MicroElectroMechanical Systems (BioMEMS). They are based on metallic wires called Planar Goubau Line (PGL). We demonstrate that high THz measurement sensitivity can be reached with new design based on spirals. But we show that the principal interest of this design is its high spatial resolution below the wavelength size compatible with living cell investigation.

1. INTRODUCTION

Microtechnology, thanks to microelectronic processes, allows to design sophisticated and miniaturized systems dedicated to biological analysis. Related dimensions enable molecular-scale or cellular-scale characterizations. These integrated devices, called BioMEMS for Biological MicroElectroMechanicalSystems, mix electronic and microfluidic functions. Their development leads to a large application field, with the opportunity to integrate new materials, technologies and sensors. Today, most of biosensors use electrochemical or optical detections, with some disadvantages. The main one is probably the probed biological-activity alteration due to the chemical reactions or the fluorescent tags bonded on molecules [1]. The radiofrequency band up to several GHz could be an interesting alternative for label-free investigations but shows a low-specificity for molecules

detection [2–4]. Nevertheless, by increasing the frequency range up to the THz spectrum, waves/photon energy reaches biological weak bonds energy, massively represented in liquids. Consequently, THz frequencies bring information concerning radicals, biomolecules but also concerning conformational states of proteins [5, 6]. Today, lot of biological studies concern protein-protein or protein-cell real-time interactions [7, 8]. THz microfluidic microsystems should be a useful tool to get sensitive and reproducible measurements in this way. To perform microscopic THz measurements, the far field approach suffers from its spatial resolution limited by diffraction. Moreover, wave-impedance matching between the propagation medium and the probed material can be difficult. To overcome the diffraction limit, the near-field approach seems to be necessary. It can be achieved by integrating planar waveguides in hyperfrequency-electronic circuits [9]. For higher frequencies, we have already demonstrated that THz propagation on metallic nano-wires is possible [10]. The combination of such a waveguide with microfluidic circuits allows us to perform THz measurements on aqueous solutions with high reproducibility and sensitivity. Until now, THz measurements on biological materials in this system have been realized in a wide spectrum to build a database. The next step presented here is the design of THz narrow-band circuits, with better sensitivity and specificity towards biological components and reactions. Nagel et al. have demonstrated that femtomolar-nucleid-acids hybridization-state can be determined by using integrated resonators [11]. The sensitivity threshold they obtained is a thousand times smaller than the one got with free space measurements. Concerning cell investigations, the difficulty is to integrate such resonators with a sufficient spatial resolution (5–50 μm) but we have demonstrate the possibility of cell culture in the microchannel of THz BioMEMS [12]. We demonstrate here that Planar Goubau Lines (PGL) technology makes it possible. In a first section, the electromagnetic propagation along planar-wire geometries is presented, with some resonance characterizations. Then, in the second section, the integrated-resonator final topology is developed. The numerous perspectives of this work are finally shown in the last section.

2. PLANAR GOUBAU LINE

The propagation around a dielectric-coated wire has been described by Goubau in 1950 [13]. Similar results are obtained with rectangular wires deposited on dielectric substrates called Planar Goubau Line (PGL) [14]. These PGL are well matched for passive THz circuits

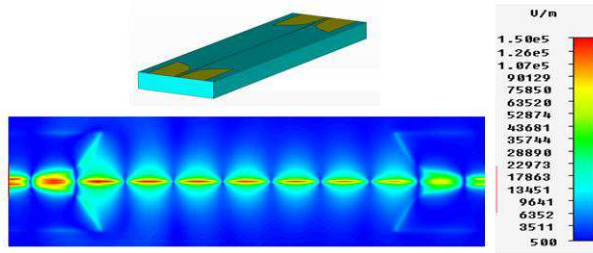


Figure 1. Computation of the electric field on the CPW-PGL-CPW circuit for a wire of 1.5 mm length and $5\ \mu\text{m}$ width at 0.18 THz on a $100\ \mu\text{m}$ quartz substrate with a titanium and gold metallization of 50/450 nm thickness respectively.

design; as microstrip lines, coplanar waveguide (CPW) or strip line (CPS) for micro and millimetric waves respectively. With PGL, THz-wave energy travels along the wire thanks to the surface electrons conduction. THz polarization is radial, in a quasi-TEM mode, and strongly confined. Indeed, study of propagation on nanometric wires (down to 100 nm) shows a micrometer-scale wave-confinement without influence on propagation parameters [10]. Experimentally, one of the main challenges concerns the Goubau mode excitation. In our case, measurements are performed with a Vectorial Network Analyzer (VNA) up to 0.325 THz coupled with coplanar tips. As a consequence, a coplanar-PGL transition has been realized to get a high-efficient Goubau mode excitation (about 75%) [15]. Figure 1 shows the electric field propagation along a 1.5 mm-long and $5\ \mu\text{m}$ -wide line, calculated with the Microwave Studio® CST 3D simulation software. The non-dispersive odd coplanar mode configuration is matched enough to realize the coupling with the quasi-TEM Goubau mode. This circuit has been used inside a microfluidic system for biological investigation on aqueous solutions and living cells [16]. The next step is the measurement sensitivity improvement around specific identified frequencies, corresponding for example to a ligand-receptor interaction. The integrated-resonator design at the micrometer-scale is the way we have chosen [17].

The main problem concerning PGL-resonator design is that there is no analytical available model yet to describe wave propagation in PGL topology. This is the reason why we have used here a simple approach based on microstrip technology model. Thus, stub-based rejectors have been designed with a $\lambda_g/4$ length (Figures 2(a) and 2(d))

where λ_g is the guided wavelength given by the well-known equation:

$$\lambda_g = \frac{c}{f_r \sqrt{\varepsilon_{reff}}} \text{ where } \varepsilon_{reff} = \frac{\varepsilon_r + 1}{2} \quad (1)$$

where f_r is the resonant frequency, ε_{reff} is the effective relative permittivity and ε_r is the substrate relative permittivity. 0.18 THz has been arbitrary chosen as the resonant frequency, which gives a 319 μm -long stub on a 100 μm -high quartz substrate ($\varepsilon_r = 4.6$; $\tan \delta = 1.10^{-4}$). Note that the finite element simulation of this geometry gives us a resonant frequency of 0.176 THz, which validates the model approximation.

Then, geometric parameters that influence on resonance quality, has been studied. In this part, CPW-PGL transition is not taken into account during computations in order to earn computing time. The electric field is only computed in the TM_{01} first Goubau mode, well described in the excitation port. In order to get smaller resonators, the stub has been folded with different configurations shown in Figure 2. To study this optimal folding, several stubs have been simulated: each one is 319 μm -long, 5 μm -wide, 1 μm -thick on a 100 μm -thick substrate. The variable parameter is the gap L and the electric fields are shown in Figures 2(d), (e), (f). Figure 2(b) shows a medium size folding which creates an interference phenomenon. This coupling is reduced when the gap between the main Goubau line and the stub becomes too small: in this case, the electric field does not distinguish the two lines (Figures 2(c) and 2(f)).

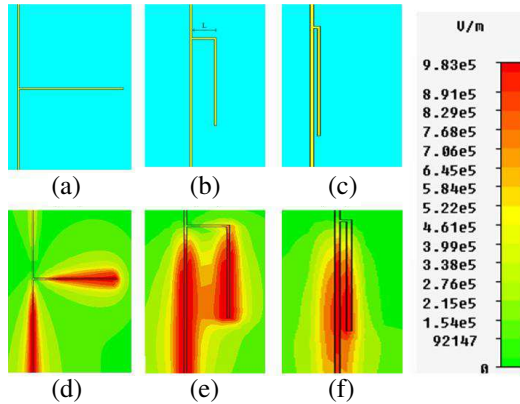


Figure 2. Different configuration of PGL stubs ((a), (b), (c)) and their computed electrical fields ((d), (e), (f)). The stub length is 319 μm for a width of 5 μm . The length bend L is equal to 65 μm ((b), (e)) and 10 μm ((c), (f)).

The shoulder L has been optimized to obtain both the integration density and the independence between the line and the stub. Figure 3(a) shows the transmission parameter for different shoulder length. We remark that when L decreases, quality factor Q increases (Figure 3(b)), because the electric field around the stub is more concentrated with a short bend length. However, L decreasing shows a resonant frequency shift to the analytical model value. The optimal L length is obtained for $L = 65 \mu\text{m}$.

Wire stub width influence has been studied (Figure 4). First observation is that the stub width does not significantly change the resonant frequency and the quality factor for values up to $20 \mu\text{m}$ ($Q = 2.5$). Over, it leads to a resonator-performance breakdown. This result is coherent with the fact that propagation losses decrease when PGL width decreases [2].

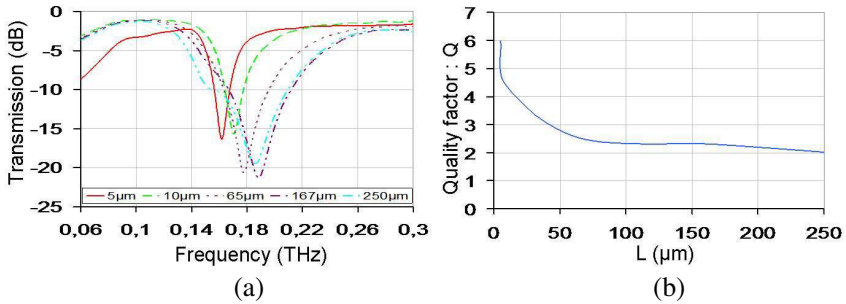


Figure 3. Spectral responses (a) and quality factors Q , (b) of PGL rejectors realized with a stub of $319 \mu\text{m}$ for different shoulder lengths.

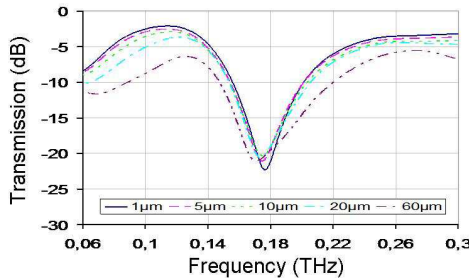


Figure 4. Spectral response of a stub of $319 \mu\text{m}$ length for different widths of wire.

3. PGL REJECTORS

The hyperfrequency-resonant structure integration is still a challenge especially with a high spatial resolution. The size of such a device must be below $100\ \mu\text{m}$, which is a typical microfluidic microchannel size. Moreover, to perform highly-sensitive THz-measurements on cells (or part of them), whose sizes are extended from $5\ \mu\text{m}$ (microglia cells) to $100\ \mu\text{m}$ (*Xenopus* oocytes), the decreasing of resonators size is the key factor.

3.1. Spiral Rejector

Considering the previous section, resonator spiral topology appears naturally. Several spiral folding configurations have been computed and their Q factor has been compared. First result is that, for a given length, the number of turns in the spiral does not influence significantly the rejector properties. The influent parameter is the spiral intrinsic gap g , which is coherent with the previous section. Moreover, study on bend corner has been led also without significant influence on the resonance. Experimentally, a 3-turn spiral has been realized and put at the middle of a 1.5 mm-long Goubau line. The spiral length has been calculated to get a resonance frequency at 0.18 THz. The spiral side size has been taken equal to $50\ \mu\text{m}$ and the spiral intrinsic gap equal to $5\ \mu\text{m}$. The whole Goubau line + spiral has been inserted between two CPW/PGL transitions to perform measurements with a VNA (Figure 5). These propagation structures have been realized on a quartz substrate thanks to 50 nm-thick titanium/450 nm-thick gold metallization and a lift off process.

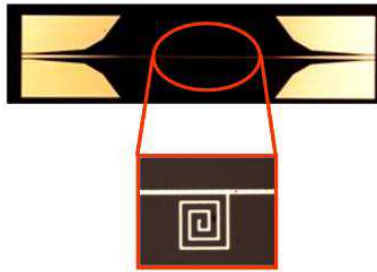


Figure 5. Example of a spiral PGL rejector realized on quartz substrate with a wire of $1500\ \mu\text{m}$ length and $5\ \mu\text{m}$ wide with two CPW-PGL transitions.

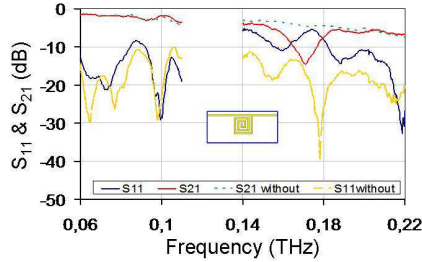


Figure 6. Experimental results obtained on the reflection parameter (S_{11}) and the transmission parameter (S_{21}) with and without (S_{21} without and S_{11} without) a three turn spiral PGL rejector realized on quartz substrate with a wire of $5\ \mu\text{m}$ wide and two CPW-PGL transitions.

Measurements were carried out with the Agilent 8510XF VNA in the 0.06–0.11 THz frequency range and a dynamic range of 58 dB at 0.11 THz and with an Anritsu 37147C associated with frequency multipliers V05VNA2-T/R from OML (Oleson Microwave Laboratories) in the 0.14–0.22 THz frequency range with Noise floor of $-77\ \text{dBm}$ and a frequency resolution of 1 kHz. Note that the lower frequency is defined by the cutoff frequency of the CPW-PGL transitions. A standard LRM (Line-Reflect-Match) calibration has been done with a Cascade Microtech XF analyzer calibration kit. Measurements of the 3-turn spiral resonator are shown in Figure 6 with a 0.172 THz rejection which well corresponds to the spiral topology.

3.2. Multiple Spiral Rejectors

3.2.1. With the Same Resonance Frequency

For improving the resonance quality, different configurations have been tested along the PGL with several 3-turn spiral resonators, as described in the Figure 7 and Figure 8. Indeed, by adding a new resonator along the wire, the quality factor can be improved. For instance, in Figure 7, four resonators alternatively located on the PGL and separated by $250\ \mu\text{m}$ give an increased rejection: $-35\ \text{dB}$ instead of $-15\ \text{dB}$ value with one single resonator. However, a resonant frequency shift appears. Figure 8 shows another configuration where the resonators are in symmetrical positions at the same place of the PGL. This configuration seems to be better for future integration into microchannels and measurements show that the quality factor is increased whereas the resonant frequency.

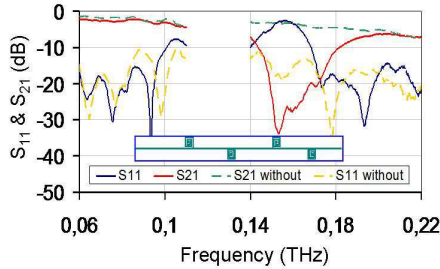


Figure 7. Spectral response of four rejectors alternatively located on PGL of 1500 μm .

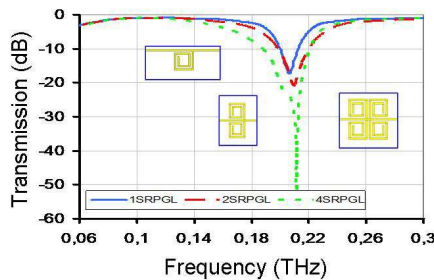


Figure 8. Spectral response of two and four rejectors combinations along the wire located at the middle of a wire of 1500 μm .

3.2.2. With Different Resonant Frequencies

The previous two-symmetric-spiral (Figure 8) configuration has also been tested with two different spiral lengths on each side of the PGL (Figure 9). This configuration could be useful for parallel biological analysis. The multiple frequency response obtained could characterize a biological solution with a better specificity and/or with multi-criteria parameters, especially when frequencies will be increased to several THz. Simulations results are shown in Figure 9. The resonator located on the PGL left side is 302.5 μm -long, whereas the other (on the right) is 240 μm -long. Resonance frequencies are clearly distinguished at 0.19 THz and 0.21 THz, with a quality factor Q equal to 10.5 and 7.5 respectively.

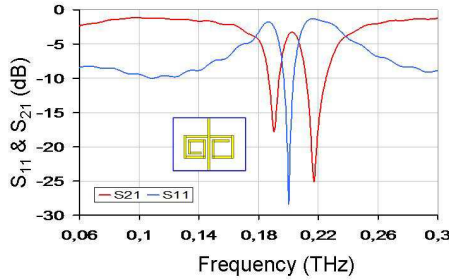


Figure 9. Spectral response of 2 rejectors centered on 0.19 and 0.21 THz respectively along the wire located at the middle of a wire of 1500 μm .

4. INTEREST AND PERSPECTIVES OF PGL REJECTORS

4.1. Potentiality in Dielectric and THz Characterization

The main interest of such circuits is to increase permittivity measurements sensitivity, for biological fine characterizations of cells for example. This is performed by integrating the previous electromagnetic functions into a microfluidic device. In this part, we have simulated the influence of liquids (located directly on the PGL-resonator) on the measured resonance. The alcohols presented in Table 1 have been tested, thanks to a second order Debye relaxation model:

$$\epsilon_r = \epsilon_\infty + \frac{\epsilon_{s1} - \epsilon_\infty}{1 + j\omega\tau_1} + \frac{\epsilon_{s2} - \epsilon_\infty}{1 + j\omega\tau_2} \quad (2)$$

where ϵ_r is the relative complex permittivity of the liquid, ϵ_∞ its the dielectric constant at very high frequency, ϵ_{s1} and ϵ_{s2} are the low frequency limits of the dielectric constant. τ_1 and τ_2 are respectively the first and second order relaxation times. Results from simulations are shown on Figures 10 and 11. First observation is that the resonant frequency shift linearly with the real part ϵ' of the permittivity. We obtain a high sensitivity at $\epsilon'/\Delta f = 108 \text{ THz}^{-1}$. Note that the frequency resolution of the VNA is $5 \cdot 10^{-5} \text{ THz}$, which so corresponds to a 0.0054 change of permittivity. Then, Q factor evolution as a function of the imaginary part ϵ'' is not linear but shows a good sensitivity too. Consequently, these first simulations show that PGL resonator is able to perform liquids permittivity characterization with a high sensitivity.

Table 1. Permittivity and relaxation parameters of various alcohols used with the second order Debye model.

Liquids	ε_{s1}	ε_{s2}	$\varepsilon_{s\infty}$	τ_1	τ_2
Methanol	32.50	5.91	2.79	51.5 ps	7.09 ps
Ethanol	24.32	4.49	2.69	163 ps	8.97 ps
1-Propanol	20.43	3.74	2.44	329 ps	15.1 ps

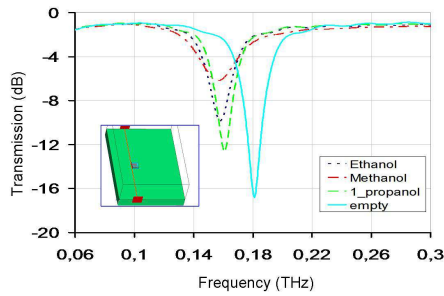


Figure 10. Spectral responses obtained on a three turn spiral PGL with different alcohols.

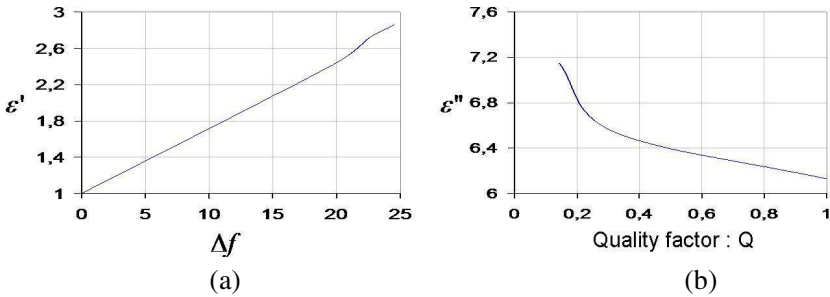


Figure 11. Evolution of frequency shifts Δf (GHz) (a) and quality factor Q, (b) with respect to respectively real and imaginary parts of the permittivity ε' and ε'' .

4.2. Perspective of This Work

The use of PGL-rejectors combined with microchannel circuits should lead to improve the biological material characterization, especially

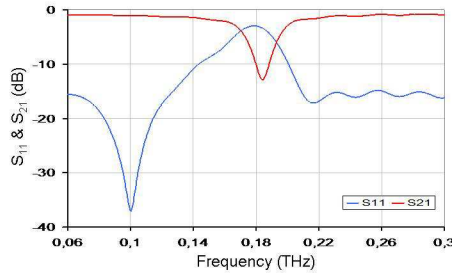


Figure 12. Spectral response of a smallest rejector of $35\ \mu\text{m} \times 35\ \mu\text{m}$ sides realized with 4 turns of $2.5\ \mu\text{m}$ width separated with a gap of $2.5\ \mu\text{m}$. We keep the same length at $315\ \mu\text{m}$ representative of the resonant frequency at $0.185\ \text{THz}$.

concerning the biological dynamical interactions. These last ones deal with protein/molecule, protein/protein, cell/protein and cell/cell relationship. Today, very few methods allow to get a real time monitoring of such interactions, and none without the use of label bounded to the biological entities. A second strong interest of such a topology is its possible integration in a microfluidic or cell handling microsystem. The previous resonator has been designed to be integrated in a $50\ \mu\text{m}$ -wide microchannel in a THz BioMEMS [16]. However, we have shown that the resonator size can be decreased again by increasing the turns number. Wire size can be thinned down to the nanometer range without strong electromagnetic-properties damage [10]. Figure 12 shows the frequency response obtained with a $2.5\ \mu\text{m}$ -wide wire, in a 4-turn spiral topology, with a $2.5\ \mu\text{m}$ gap. The corresponding spiral-side size is equal to $35\ \mu\text{m}$. This simulation proves that it is possible to optimize the rejectors dimension depending on the probed-biological-entity size.

The third interest of PGL resonator is their potential use up to the THz and far infrared spectrum. Indeed, a $58\ \mu\text{m}$ -long resonator has been simulated and shows a $1.08\ \text{THz}$ resonant frequency (Figure 13). THz spectroscopy has demonstrated its interest in biological characterization, especially on dehydrated materials. This measurement methodology is inspired from X-ray crystallography and is the consequence of the huge water absorption of T-rays. More recently THz-instrumentation improvements lead to measurements on liquid-solutions and show abilities to characterize protein conformation states. This is why we couple micro-nanotechnology and THz spectroscopy with the use of waveguides inside microfluidic circuits [6, 8].

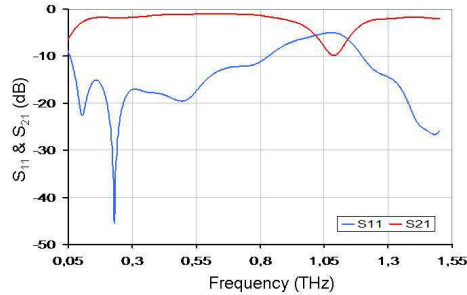


Figure 13. Spectral response of a smallest retractor of $18 \mu\text{m} \times 18 \mu\text{m}$ sides realized with 1 turns separated with a gap of $2.5 \mu\text{m}$ and a wire of $5 \mu\text{m}$ width. We change the length at $58 \mu\text{m}$ for obtaining a resonant frequency at 1.08 THz.

5. CONCLUSION

This work has shown that PGL topology is very well adapted to design integrated planar waveguides in the THz range. It could benefit from interferometers and resonators to improve measurements sensitivity. Indeed, THz PGL-rejectors have been successfully realized with a simple spiral design. The obtained features are comparable to the ones obtained by other topologies such as Split Ring Resonator for example. The main advantage of the spiral design is the possibility to dramatically decrease the resonator size down to the micrometer range. This property allows us to use these devices inside microsystems dedicated to biological characterizations. The realized THz small and passive device resonator is compatible with the microchannel size. Note that THz spectroscopy is the emergent technology in this topic because of its direct low-energy-binding probing. In a more original way, we think that these resonators can be used to perform living cell characterizations. Future THz biochips should also benefit from the power dividers or couplers development.

ACKNOWLEDGMENT

The authors gratefully acknowledge the Ministry and the University Lille1 through the Interdisciplinary Research Program PPF BioMEMS 2006–2010, No. 1803.

REFERENCES

1. Facer, G. R., D., A. Notterman, and L. L. Sohn, "Dielectric spectroscopy for bioanalysis: From 40 Hz to 26.5 GHz in microfabricated wave guide," *Applied Physics Letters*, Vol. 78, No. 7, 996–998, 2001.
2. Treizebre, A., T. Akalin, and B. Bocquet, "Planar excitation of Goubau Line for THz BioMEMS," *IEEE Microwave and Wireless Components Letters*, Vol. 15, No. 12, 886–888, 2005.
3. Li, L. J., "Simultaneous detection of organic and inorganic substances in a mixed aqueous solution using a microwave dielectric sensor," *Progress In Electromagnetics Research C*, Vol. 14, 163–171, 2010.
4. Dalmay, C., M. Cheray, A. Pothier, F. Lallou, M. O. Jauberteau, and P. Blondy, "Ultra sensitive biosensor based on impedance spectroscopy at microwave frequencies for cell scale analysis," *Sensors and Actuators A: Physical*, Vol. 162, No. 2, 189–197, 2010.
5. Born, B. and M. Havenith, "Terahertz dance of proteins and sugar with water," *International Journal of Infrared and Millimeter Waves*, Vol. 13, 1245–1254, 2009.
6. Laurette, S., A. Treizebre, F. Affouard, and B. Bocquet, "Subterahertz characterization of ethanol hydration layers by microfluidic system," *Applied Physics Letters*, Vol. 97, No. 11, 111904-1–111904-3, 2010.
7. George, P. A., W. Hui, F. Rana, B. G. Hawkins, A. E. Smith, and B. J. Kirby, "Microfluidic devices for terahertz spectroscopy of biomolecules," *Optics Express*, Vol. 16, No. 3, 1577–1582, 2008.
8. Abbas, A., A. Treizebre, P. Supiot, N. E. Bourzgui, D. Guillochon, D. Vercaigne-Marko, and B. Bocquet, "Cold plasma functionalized TeraHertz BioMEMS for enzyme reaction analysis," *Biosensors and Bioelectronics*, Vol. 25, No. 1, 154–160, 2009.
9. Gupta, K. C., *Microstrip Lines and Slotlines*, 2nd edition, Artech House, Boston, 1996.
10. Treizebre, A. and B. Bocquet, "Nanometric metal wire as a guide for THz investigation of living cells," *International Journal of Nanotechnology*, Vol. 5, No. 6–8, 784–795, 2008.
11. Nagel, M., P. H. Bolivar, M. Brucherseifer, H. Kurz, A. Bossert-Hoff, and R. Buttner, "Integrated planar terahertz resonators for femtomolar sensitivity label-free detection of DNA hybridization," *Applied Optics*, Vol. 41, No. 10, 2074–2078, 2002.
12. Treizebre, A., B. Bocquet, D. Legrand, and J. Mazurier, "THz microscopic investigation on living cells," *Proceeding*

- International Conference on Microtechnologies in Medicine and Biology*, Canada, April 1–3, 2009.
13. Goubau, G., “Open wire lines,” *IEEE Microwave Theory and Techniques*, Vol. 4, No. 4, 197–200, 1956.
 14. Xu, Y. and R. G. Bosisio, “A comprehensive study on the planar type of Goubau line for millimetre and submillimetre wave integrated circuits,” *IET Microwaves, Antennas and Propagation*, Vol. 1, No. 3, 681–687, 2007.
 15. Treizebre, A., B. Bocquet, Y. Xu, and R. G. Bosisio, “New THz excitation of planar goubau line,” *Microwave and Optical Technology Letters*, Vol. 50, No. 11, 2988–3001, 2008.
 16. Treizebre, A., B. Bocquet, D. Legrand, and J. Mazurier, “Studies of cellular informative transfer by THz BioMEMS,” *Proceedings of International Conferences on Infrared Millimeter and Terahertz Wave (IRMMW-THz 2008)*, California, September 15–19, 2008.
 17. Wang, B. and G. P. Wang, “Plasmonic waveguide ring resonator at terahertz frequencies,” *Applied Physics Letters*, Vol. 89, No. 13, 1331006-1–1331006-3, 2006.